Physica B 717 (2025) 417762

Contents lists available at ScienceDirect

Physica B: Condensed Matter

journal homepage: www.elsevier.com/locate/physb

Time resolved core level spectroscopy reveals light-induced structural changes in $GdTe_3$

Martina Dell'Angela [a,*], Roberto Costantini [a,b], Alberto Morgante [a,b], Anisha Singh [c,d], Ian R. Fisher [c,d], Giancarlo Panaccione [a], Federico Cilento [e,*]

[a] CNR - Istituto Officina dei Materiali (IOM), Area Science Park, Strada Statale 14, Km 163.5, Trieste, 34149, Italy
[b] Dipartimento di Fisica, Università di Trieste, Via Valerio 2, Trieste, 34127, Italy
[c] Stanford Institute for Materials and Energy Sciences, SLAC National Accelerator Laboratory, Menlo Park, 94025, CA, USA
[d] Department of Applied Physics, Stanford University, Stanford, 94305, CA, USA
[e] Elettra - Sincrotrone Trieste S.C.p.A, Strada Statale 14, Km 163.5, Trieste, 34149, Italy

ARTICLE INFO

Keywords:
Time resolved photoemission
Charge density waves
Pump–probe at synchrotron
Transient states

ABSTRACT

Complex materials frequently exhibit broken symmetry phases, driven by a delicate balance of electronic, lattice, spin and orbital anisotropies. In this context, new phases of matter may emerge when this equilibrium is disturbed by photoexcitation. Here we investigate the response to ultrafast optical excitation of the $GdTe_3$ charge density wave (CDW) compound, by time-resolved X-ray photoemission spectroscopy (TR-XPS). By measuring the energy separation between two atomic species of Te 4d core levels, we identify a sharp discontinuity occurring precisely at the CDW transition temperature, confirming the sensitivity of this technique to the onset of the CDW order. Optical excitation with a novel Echelon-based pulse-replication scheme reveals the formation of a third low-valence tellurium specie, absent under equilibrium conditions, indicative of a light-induced structural rearrangement. The study provides new information on the rich dynamics in $GdTe_3$ and opens new avenues for research in this field by using TR-XPS at synchrotron sources.

1. Introduction

The family of rare-earth (R) tritellurides, RTe_3, exhibits a rich phenomenology of unidirectional and bidirectional incommensurate charge density waves (CDWs) [1,2]. These have been intensively studied in the past few decades, drawing renewed interest due to the demonstration that a peculiar orthogonally-rotated light-induced CDW state can be obtained in $LaTe_3$ and $CeTe_3$ [3–5]. RTe_3 materials generally exhibit at least one incommensurate unidirectional CDW state, with critical temperature T_{c1} ranging between 240 K (for R=Tm) and 670 K (for R=La), oriented along the *c*-axis (c > a by ≈0.1%) [6]. The CDW ordering has been observed by a variety of experimental techniques [1,7–10] and its formation appears to be driven by a strongly momentum-dependent electron–phonon coupling [11,12]. T_{c1} can be tuned by changing the rare earth element, that sets the internal chemical pressure [13], or by applying external pressure [14]. In some RTe_3, a second orthogonal CDW phase (along the *a*-axis) emerges, with a lower critical temperature T_{c2}, ranging from 40 K (for R=Tb) [15] to 180 K (for R=Tm), indicating that the two equilibrium CDWs are in competition [13,16]. Photoexcitation typically melts the equilibrium CDW state [17,18], and in some cases, like $LaTe_3$ and $CeTe_3$, can induce a transient non-equilibrium CDW along the *a*-axis, lasting for a few picoseconds. This transition is associated to topological defects formed by the local absorption of high-energy photons, that suppress the *c*-axis CDW and allows an *a*-axis CDW (the *a* axis CDW being normally forbidden). While these defects are localized, the transient CDW phase can appear over a wide sample area, generating transient quantum states and a proliferation of topological defects. Recent studies have demonstrated that anisotropic in-plane strain can also rotate the equilibrium CDW wavevector from the *c*-axis to the *a*-axis [19–21].

We consider $GdTe_3$, having an orthorhombic crystal structure with Cmcm space symmetry with two R-Te slabs separated by two Te sheets, allowing easy exfoliation [1]. $GdTe_3$ exhibits high electron mobility and good conductivity, making it promising for applications such as supercapacitors and spintronics [22]. It presents a unidirectional CDW along the *c*-axis below 377 K and no *a*-axis CDW [13]. The possibility of inducing a transient CDW phase along the transverse direction is currently under debate: optical pumping can drive the lattice to a quasi-equilibrium state that persists for nanoseconds, though this transition requires surpassing a threshold fluence and remains athermal [23]. Despite the absence of an observed transient *a*-axis CDW, scanning

* Corresponding authors.
E-mail addresses: dellangela@iom.cnr.it (M. Dell'Angela), federico.cilento@elettra.eu (F. Cilento).

https://doi.org/10.1016/j.physb.2025.417762
Received 13 June 2025; Received in revised form 29 August 2025; Accepted 30 August 2025
Available online 18 September 2025

tunneling microscopy studies suggest that localized *a*-axis CDWs might form near twin domain boundaries due to dislocations, where competing *c*-axis and *a*-axis domains intersect [24]. In this study, we combine temperature-dependent core level X-ray photoelectron spectroscopy (XPS) measurements on $GdTe_3$ and $TbTe_3$ single crystals with time-resolved X-ray photoelectron spectroscopy (TR-XPS) on $GdTe_3$, performed at the ANCHOR-SUNDYN endstation [25] at the Elettra synchrotron (Trieste, Italy).

Core level XPS is a powerful technique for analyzing local charge changes due to CDWs, as it was shown for the transition metal dichalcogenides, where the chemical shift of the core level binding energies is due to the presence of inequivalent sites [26]. Previous studies have revealed CDW dynamics in TaS_2 using time-resolved XPS measurements at free electron laser [27,28] and synchrotron sources [29]. CDW signatures in lanthanum tritellurides, particularly in the Te core level spectra, remain poorly understood, with peak assignments still debated and CDW melting unexplored [30–32]. Here, we use core level XPS to investigate the CDW melting in $GdTe_3$. By analyzing the Te 4d XPS spectra when the temperature is increased across the CDW transition in $GdTe_3$ and $TbTe_3$, we observe a discontinuity in the energy splitting between two Te components (assigned to the two inequivalent Te atoms in the unit cell) and recognize it as the fingerprint of the CDW phase transition. Moreover, by using a novel excitation scheme, we performed an optical pump–synchrotron probe XPS study revealing the sub-nanosecond dynamics of the Te 4d lines, offering a new perspective on the athermal excited state. Here, we demonstrate the viability of a novel experimental approach using an Echelon excitation scheme to investigate transient states of matter at synchrotron facilities with ≈100 ps-long X-ray pulses.

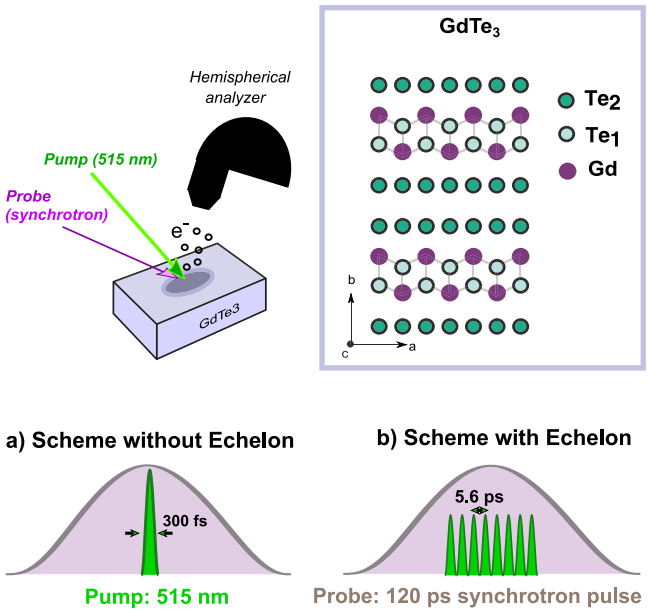

Fig. 1. Schematic of the experimental setup, showing the two beams incident on the sample and the hemispherical analyzer. The sample crystal structure is also reported with the identification of the inequivalent Te atoms as Te_1 (light green) and Te_2 (dark green). Panels a) and b) schematically illustrate the pump and probe pulses, with panel b) highlighting the pump pulse replication achieved by introducing the Echelon device.

2. Experimental

X-ray photoemission measurements were conducted at the ANCHOR-SUNDYN endstation [25] of the ALOISA beamline at the Elettra synchrotron radiation facility (Italy). $GdTe_3$ and $TbTe_3$ single crystals have been grown by slow-cooling a Te-rich melt (i.e. by a self-flux technique, as reported previously [6,13,33]), followed by decanting in a centrifuge in Stanford and transported in oxygen-free vials between the laboratories. The crystals used in this work have approximate dimensions of 2 mm × 2 mm. They have been glued to the sample holder in a N_2-purged glove box, using a bi-component silver epoxy, and then transferred to the UHV system, minimizing the exposure to air. Once inserted in the UHV apparatus, the crystals have been cleaved with kapton tape at pressures better than 5×10^{-10} mbar, to prepare the surface for the experiments. The cleanliness of the samples, including the absence of contaminants and potential oxidation, was confirmed via XPS wide scans. All XPS measurements were performed using a Phoibos 150 hemispherical electron analyzer.

The XPS measurements as a function of sample temperature on $GdTe_3$ and $TbTe_3$ have been performed in sweep mode, setting a photon energy of 320 eV and 20 eV pass-energy (PE). The sample temperature was increased in 10 K steps and the temperature control in UHV environment was achieved through PID-controlled radiative heating.

Pump–probe XPS experiments were performed on $GdTe_3$ samples. These measurements employed an optical laser beam as a pump and the synchrotron beam as a probe, arranged in a quasi-collinear geometry. The output of a Tangerine HP (Amplitude Systemes) amplified laser system was frequency doubled at 515 nm. The laser was operated at repetition rates of either 385.67 kHz or 192.83 kHz. The fluence deposited on the sample was approximately 0.2 mJ/cm^2 at both repetition rates, using a spot diameter of 300 μm FWHM, comparable to the synchrotron probe. The pump fluence was maintained below levels causing irreversible sample changes due to average heating. The Elettra synchrotron was operated in hybrid mode, delivering a multibunch pulse pattern at 499.654 MHz with an isolated X-ray pulse at 1.157 MHz repetition rate. The acquisition was performed by simultaneously measuring the electrons emitted from the excited sample by the pumped X-ray pulse and from the reference unexcited condition provided by the probe pulse at long delay (864 ns), as detailed in the Supporting information material. The electron analyzer was operated in fixed mode at PE=30 eV and all the spectra have been corrected for the detector inhomogeneity. The time resolved XPS measurements have been conducted by synchronizing the pump and probe beams with a phase shifter and then scanning a delay stage around time zero to enhance the signal statistics. The zero time-delay was determined by measuring surface photovoltage effects on the Si 2p levels of a silicon sample.

A schematic of the experimental setup is illustrated in Fig. 1. Two experimental configurations were employed: a conventional pump–probe, illustrated in panel a) of Fig. 1, and an ad-hoc built setup, sketched in panel b) of Fig. 1, that makes use of an Echelon device inserted into the pump beam path. This modification generates multiple pump pulse replicas (≈8) with 5.6 ps separation (see Supporting information material), leading to repeated excitation of the sample. As a result, the probability of probing the excited state is significantly enhanced, particularly when a long-duration probe pulse is used. For the experiments in the two configurations, the same incident average power was set. Hence, in the case of the Echelon configuration, a lower fluence is set, because of the pulse replication. Considering that the excited state lifetime measured via time-resolved diffraction measurements on $GdTe_3$ is approximately 5 ps [23] (the optical pump pulse has a duration of 300 fs), whereas the synchrotron pulse lasts for 120 ps, it descends that only a small portion of the X-ray pulse captures the excited state in the standard configuration (Fig. 1a)). Conversely, the use of an Echelon device enhances the interaction time-window, rendering the effect more pronounced.

3. Results and discussion

We first studied the evolution of the lineshape of the Te 4d core level lines of $GdTe_3$ and $TbTe_3$ when the sample temperature T is driven

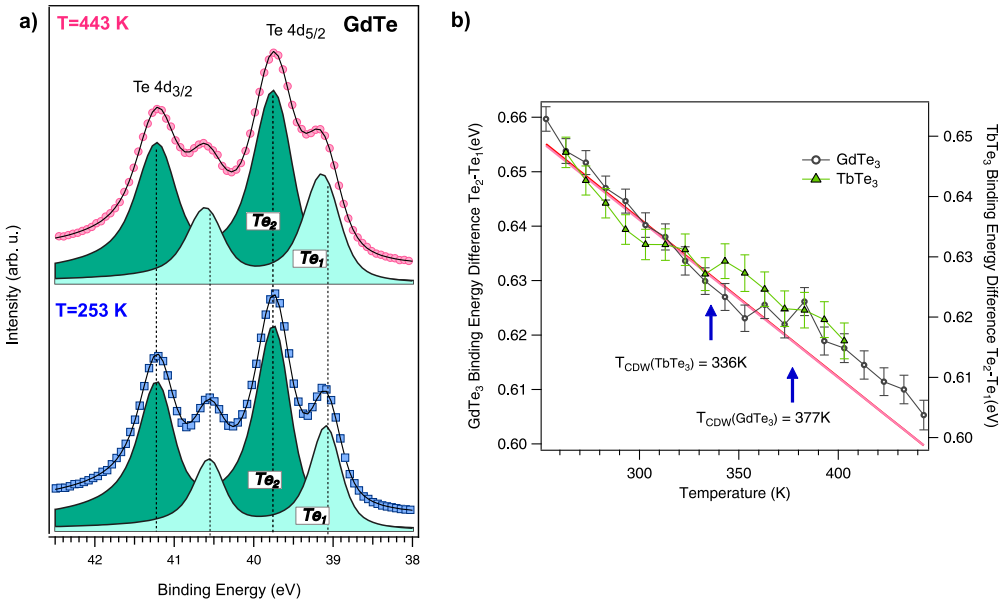

Fig. 2. a) Te 4d core level lines measured with 320 eV photon energy on $GdTe_3$ at T=253 K (red dots) and T=443 K (blue squares). The best fit to the data with two DS lineshapes and the peak deconvolution is also reported below each spectrum. The vertical dot–dash lines indicate the fitted peak positions of the two chemically distinct Te components at 253 K. These lines serve as a reference to highlight the temperature-dependent shifts of these peaks observed at higher temperatures. b) Binding energy difference between the two chemically distinct Te 4d components (Te_1 and Te_2) as a function of sample temperature for $GdTe_3$ and $TbTe_3$. The temperatures from the literature of the CDW transition are also reported on the graph [13].

across the CDW critical temperature of the two samples. Afterward, we measured the dynamics of the Te 4d lines of $GdTe_3$ during the light-induced melting of the CDW, on the sub-nanosecond timescale.

Fig. 2 a) shows the Te 4d core level spectrum of $GdTe_3$ measured with 320 eV photon energy and the sample at T=253 K (red dots) and T=443 K (blue squares). Two components of the spin–orbit split Te $4d_{5/2}$ and $4d_{3/2}$ peaks can be identified in each spectrum. They are labeled Te_1 and Te_2 and obtained by the best fit of the data with two Donjach-Šunjić (DS) pairs as shown at the bottom of each trace. All the spectra have been aligned with the Te_2 components at 39.75 eV to account for energy drifts. Following the assignments in ref [31], we attribute the Te_1 component to the Te atoms in the GdTe slab, while the Te_2 component is contributed by the Te atoms in the Te–Te sheets (see Fig. 1). This assignment is also supported by the 1:2 intensity ratio between Te_1 and Te_2.

Fig. 2 b) shows the energy difference between the positions of the Te_1 and Te_2 components as a function of sample temperature. The peak separation has been obtained by fitting the Te 4d photoemission lines, as described in Fig. 2 a). In these fits, the intensity, position and Gaussian broadening of the DS pairs were treated as free parameters. The peak separation decreases linearly with the temperature T, at a rate of 2.9×10^{-4} eV/K. Notably, a sharp discontinuity in the energy difference between the Te_1 and Te_2 components in $GdTe_3$ occurs precisely at the CDW transition temperature $T_{CDW}(GdTe_3)$=377 K, as marked by the blue arrow in Fig. 2 b). This linear decrease in T can be attributed to the extreme sensitivity of core level shifts to the lattice expansion [34], while the discontinuity indicates the onset of the CDW phase transition. To test the generality of this behavior, we repeated the same experiment on $TbTe_3$, which has a $T_{CDW}(TbTe_3)$ of 336 K. The results are shown in Fig. 2 b). Similar to the case of $GdTe_3$, we observe a linear decrease in the spacing between the two Te components, with a coefficient of 2.6×10^{-4} eV/K, and a discontinuity in the energy difference occurring precisely at the CDW transition temperature. This finding unambiguously identifies the discontinuity as a fingerprint of the CDW phase transition in tritellurides.

Additionally, we observe that below the CDW transition, the separation between the two components is larger for the heavier compounds. This result aligns with previously reported spectra for $ErTe_3$ and $PrTe_3$ [32], where the Te_1 and Te_2 separation is larger for Pr than for Er. Combining all these observations, we identify the discontinuity in the separation between the Te_1 and Te_2 components as indicator of the CDW transition.

After confirming that the Te 4d core level lines exhibit distinctive features indicative of the CDW transition, we proceeded to measure its dynamics to study the photoexcited state. Pump–probe photoemission was conducted using 2.4 eV (515 nm) pump pulses, synchronized with the hybrid bunch at the Elettra synchrotron. We focused on analyzing the dynamics within a time range of 300 ps centered around time zero. Figs. 3 b) and c) show the difference maps, acquired without and with the Echelon device respectively. These maps were obtained by measuring the Te 4d XPS spectrum at different pump–probe delays and subtracting, for each measurement, the late delay reference spectra (see Supplementary information A.1).

Fig. 3 a) shows the two Te 4d reference spectra from Fig. 2, acquired at two different temperatures (T=253 K and T=443 K), along with the Te 4d late delay spectrum measured at T=253 K. This spectrum exhibits broadening due to both the pump-induced average heating and the larger analyzer pass energy (see Experimental methods). All the spectra have been aligned with the Te_2 components at 39.75 eV to account for energy drifts. In both Figs. 3 b) and c), we observe strong intensity variations around zero pump–probe delay. Considering the synchrotron pulse duration is ≈120 ps, we integrated the two maps over the entire delay window. The resulting differential spectra are plotted in Figs. 3 e) and f) (filled areas). The late delay spectrum is always shown with a dashed line and serves as a reference for the XPS lineshape.

Fig. 3 d) shows a differential spectrum obtained from spectra acquired at two temperatures across T_{CDW}, as shown in Fig. 3 a). This curve represent the temperature-induced change in the XPS lineshape at equilibrium. The differential spectra reported in Figs. 3 e) and f) indicate that photoexcitation induces a non-equilibrium signal that markedly differs with respect to the effect of simple heating, and that also varies depending on the excitation scheme used. In Fig. 3 e), the difference spectrum obtained without pulse replication can be explained by considering pump-induced vacuum space charge effects on the photoemission signal, which cause a rigid shift of the spectrum [35,36]. This effect has been simulated (as shown by the green

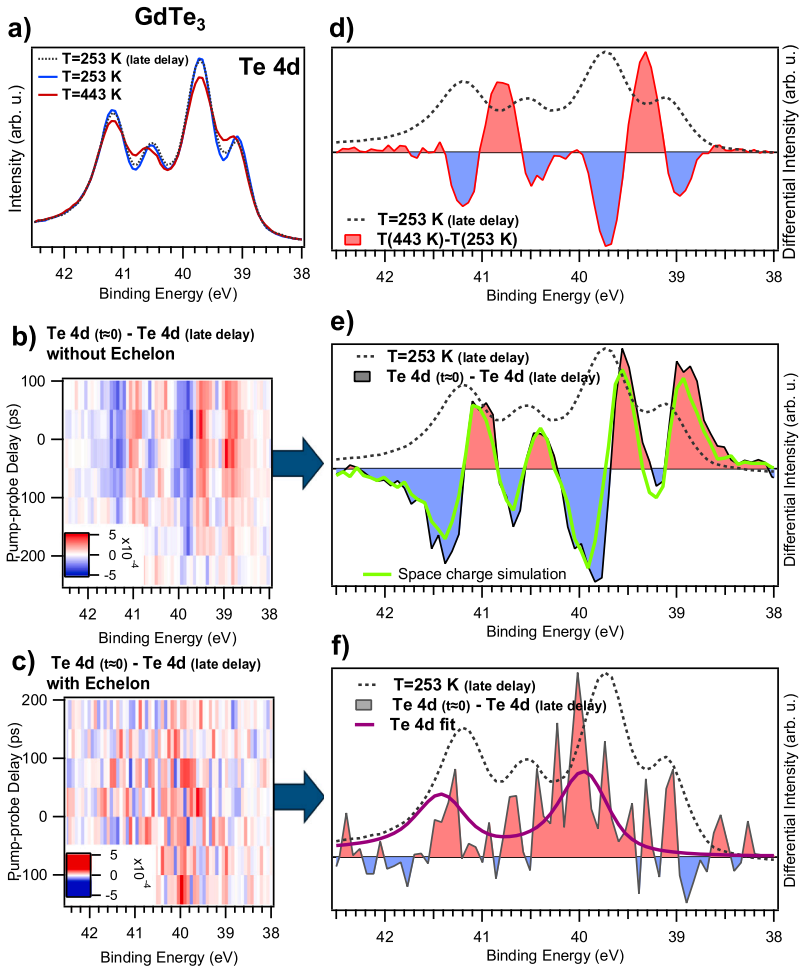

Fig. 3. Dynamics of the Te 4d core level lines. (a) Te 4d reference spectra at two different temperatures, along with the spectrum measured with pump on at a late delay of 864 ns, showing broadening due to experimental conditions. All Te_2 spectra are aligned to 39.75 eV. (b) and (c) Difference maps with and without the Echelon device, obtained by subtracting spectra acquired at a late delay from those measured at various pump–probe delays in a 300 ps region around time zero. (d) Differential spectrum at two temperatures across the CDW transition. (e) Differential spectrum without pulse replication, displaying a rigid shift due to pump-induced vacuum space charge effects (green line: simulated spectrum). (f) Differential spectrum with the Echelon device, showing a positive residual on the high-energy side of the Te_1 component and an additional DS component (red line) at 39.9 eV.

line) by subtracting a spectrum obtained by shifting the late delay reference spectrum by 20 meV from itself. Conversely, the difference spectrum shown in Fig. 3 f), obtained with the Echelon device, does not exhibit any vacuum space charge effect. Instead, it displays a positive residual signal on the high-energy side of the Te_2 component. This signal can be modeled with an additional DS component (purple line) at 39.9 eV (0.15 eV shift with respect to the Te_2), with an intensity of about 0.5% of the Te_1 component and the same fixed intensity ratio of the multiplet peaks. This model and the 0.5% value should be regarded as only indicative because the XPS intensity on the core level should in principle be conserved. However, factors such as photoelectron diffraction, scattering effects, and the fixed detection geometry prevent a strict quantitative conservation analysis in the transient regime. The additional component in the Te lines, appearing on the high-binding energy side of the Te_2 component, cannot be attributed to thermal effects, whose fingerprint is displayed in Fig. 3 d), and which are likely associated to a lattice expansion. Furthermore, the intensity variation observed with the Echelon device differs from the effect associated to the CDW transition, which corresponds to an increase in peak separation. Hence, we infer that the observed transient signal describes a novel excited state and we are currently running further investigations to explain the behavior. This novel state of matter might represent a precursor state with altered lattice parameters, that eventually favors the emergence of the rotated light-induced CDW state in the highest Tc compounds, where a balance of external (light-induced) and internal pressure might set favorable conditions for the emergence of the rotated CDW state. An anisotropic lattice expansion [20,37] after light excitation indeed might be at the origin of the transient switch of the relative length of the a and c lattice parameters, that leads to the formation of the transient rotated CDW state. Microscopically, the new peak signals a Te environment with modified (reduced) valence, that emerges after a charge transfer away from Te.

4. Conclusion

In this work we combined XPS and Time-Resolved XPS at the Elettra Synchrotron in order to disclose the fingerprints of the CDW transition in $GdTe_3$ and $TbTe_3$ on their Te 4d core level lines, and the effect of photoexcitation in the case of $GdTe_3$. We found that the energy separation of the XPS peaks associated to the two Te species of RTe_3 linearly decreases as the temperature is increased. Importantly, this trend shows a discontinuous jump taking place exactly at T_{CDW}, providing a clear fingerprint of the onset of the CDW phase. Conventional photoexcitation of $GdTe_3$ at moderate fluence displays a modification of the XPS lineshape that can be linked to a space-charge effect, that hides the underlying physical modification to the 4d Te pekas. Using an Echelon-based excitation scheme instead, the modification to the 4d Te

peaks can be revealed. Photoexcitation triggers the formation of a third Te specie with smaller valence and amounting to 0.5% of the Te weight. This new component indicates a light-induced reversible formation of a long-lived state with non-thermally modified lattice parameters. In conclusion, our work proves the viability of a new protocol for the study of transient states of matter at Synchrotron sources with ≈ 100 ps long X-ray pulses, and discloses the light-induced formation of a novel reversible state in $GdTe_3$, that might be of importance for the understanding of the rich phenomenology of the multiple CDW states in RTe_3 compounds.

CRediT authorship contribution statement

Martina Dell'Angela: Writing – original draft, Methodology, Investigation, Funding acquisition, Data curation, Conceptualization. **Roberto Costantini:** Writing – review & editing, Methodology, Investigation. **Alberto Morgante:** Writing – review & editing. **Anisha Singh:** Methodology, Investigation. **Ian R. Fisher:** Writing – review & editing, Methodology. **Giancarlo Panaccione:** Writing – review & editing. **Federico Cilento:** Writing – original draft, Methodology, Investigation, Conceptualization.

Declaration of competing interest

The authors declare that they have no known competing financial interests or personal relationships that could have appeared to influence the work reported in this paper.

Acknowledgments

Crystal growth at Stanford University was supported by the Department of Energy, Office of Basic Energy Sciences, under contract DE-AC02-76SF00515. MDA acknowledges financial support under the National Recovery and Resilience Plan (NRRP), Mission 4, Component 2, Investment 1.1, Call for tender No. 104 published on 2.2.2022 by the Italian MUR, funded by the European Union – NextGenerationEU – Project MEGS – CUP B53D23003930006. RC, AM and GP carried out this study within the NQSTI and received funding from Next-GenerationEU (Piano Nazionale di Ripresa e Resilienza (PNRR) - Missione 4, Componente 2, Investimento 1.3-PE00000023).

Appendix A. Supplementary data

Supplementary material related to this article can be found online at https://doi.org/10.1016/j.physb.2025.417762.

Data availability

Data will be made available on request.

References

[1] K. Yumigeta, Y. Qin, H. Li, M. Blei, Y. Attarde, C. Kopas, S. Tongay, Advances in rare-earth tritelluride quantum materials: Structure, properties, and synthesis, Adv. Sci. 8 (12) (2021) 1–17, https://onlinelibrary.wiley.com/doi/10.1002/advs.202004762.

[2] V. Brouet, W.L. Yang, X.J. Zhou, Z. Hussain, R.G. Moore, R. He, D.H. Lu, Z.X. Shen, J. Laverock, S.B. Dugdale, N. Ru, I.R. Fisher, Angle-resolved photoemission study of the evolution of band structure and charge density wave properties in RTe_3. (R=Y, La, Ce, Sm, Gd, Tb, and Dy), Phys. Rev. B 77 (2008) 235104, https://link.aps.org/doi/{10}.1103/{PhysRevB}.77.235104.

[3] A. Kogar, A. Zong, P. Dolgirev, X. Shen, J. Straquadine, Y. Bie, X. Wang, T. Rohwer, I. Tung, Y. Yang, R. Li, J. Yang, S. Weathersby, S. Park, M. Kozina, E. Sie, H. Wen, P. Jarillo-Herrero, I. Fisher, X. Wang, N. Gedik, Light-induced charge density wave in $LaTe_3$, Nat. Phys. 16 (2020) 159–163, http://dx.doi.org/10.1038/s41567-019-0705-3.

[4] F. Zhou, J. Williams, S. Sun, C. Malliakas, M. Kanatzidis, A. Kemper, C. Ruan, Nonequilibrium dynamics of spontaneous symmetry breaking into a hidden state of charge-density wave, Nat. Commun. 12 (2021) 566, http://dx.doi.org/10.1038/s41467-020-20834-5.

[5] A. Zong, A. Kogar, Y.-Q. Bie, T. Rohwer, C. Lee, E. Baldini, E. Ergeçen, M.B. Yilmaz, B. Freelon, E.J. Sie, H. Zhou, J. Straquadine, P. Walmsley, P.E. Dolgirev, A.V. Rozhkov, I.R. Fisher, P. Jarillo-Herrero, B.V. Fine, N. Gedik, Nat. Phys. 15 (1) (2019) 27–31, http://dx.doi.org/10.1038/s41567-018-0311-9.

[6] N. Ru, J.-H. Chu, I.R. Fisher, Magnetic properties of the charge density wave compounds RTe_3 (R=Y, La, Ce, Pr, Nd, Sm, Gd, Tb, Dy, Ho, Er, and Tm), Phys. Rev. B 78 (2008) 012410, http://dx.doi.org/10.1103/PhysRevB.78.012410.

[7] E. DiMasi, M.C. Aronson, J.F. Mansfield, B. Foran, S. Lee, Chemical pressure and charge-density waves in rare-earth tritellurides, Phys. Rev. B 52 (1995) 14516, http://dx.doi.org/10.1103/PhysRevB.52.14516.

[8] A. Fang, N. Ru, I.R. Fisher, A. Kapitulnik, Scanning tunneling microscopy study of charge density wave structure in $TbTe_3$, Phys. Rev. Lett. 99 (2007) 046401, http://dx.doi.org/10.1103/PhysRevLett.99.046401.

[9] B. Hu, A.F. Fang, N. Ru, I.R. Fisher, N.L. Wang, Optical spectroscopy study on RTe_3, Phys. Rev. B 89 (2014) 075140, http://dx.doi.org/10.1103/PhysRevB.89.075140.

[10] M. Lavagnini, A. Sacchetti, L. Degiorgi, N. Ru, I.R. Fisher, Raman scattering study of lattice dynamics in RTe_3 (R=La, Ce, Pr, Nd, Sm, Gd, Dy), Phys. Rev. B 77 (2008) 165132, http://dx.doi.org/10.1103/PhysRevB.77.165132.

[11] M. Maschek, S. Rosenkranz, R. Heid, A. Said, P. Giraldo-Gallo, I. Fisher, F. Weber, Wave-vector-dependent electron–phonon coupling and the charge-density-wave transition in $TbTe_3$, Phys. Rev. B 91 (2015) 235146, https://link.aps.org/doi/10.1103/PhysRevB.91.235146.

[12] M. Johannes, I. Mazin, Fermi surface nesting and the origin of charge density waves in metals, Phys. Rev. B 77 (2008) 165135, https://link.aps.org/doi/10.1103/PhysRevB.77.165135.

[13] N. Ru, C. Condron, G. Margulis, K. Shin, J. Laverock, S. Dugdale, M. Toney, I. Fisher, Effect of chemical pressure on the charge density wave transition in rare-earth tritellurides RTe_3, Phys. Rev. B 77 (2008) 035114, https://link.aps.org/doi/10.1103/PhysRevB.77.035114.

[14] A. Sacchetti, C. Condron, S. Gvasaliya, F. Pfuner, M. Lavagnini, M. Baldini, M. Toney, M. Merlini, M. Hanfland, J. Mesot, J. Chu, I. Fisher, P. Postorino, L. Degiorgi, Pressure-induced quenching of the charge-density-wave state in rare-earth tritellurides observed by x-ray diffraction, Phys. Rev. B 79 (2009) 201101, https://link.aps.org/doi/10.1103/PhysRevB.79.201101.

[15] A. Banerjee, Y. Feng, D. Silevitch, J. Wang, J. Lang, H. Kuo, I. Fisher, T. Rosenbaum, Charge transfer and multiple density waves in the rare earth tellurides, Phys. Rev. B 87 (2013) 155131, https://link.aps.org/doi/10.1103/PhysRevB.87.155131.

[16] R. Moore, V. Brouet, R. He, D. Lu, N. Ru, J. Chu, I. Fisher, Z. Shen, Fermi surface evolution across multiple charge density wave transitions in $ErTe_3$, Phys. Rev. B 81 (2010) 073102, https://link.aps.org/doi/10.1103/PhysRevB.81.073102.

[17] M. Trigo, P. Giraldo-Gallo, J. Clark, M. Kozina, T. Henighan, M. Jiang, M. Chollet, I. Fisher, J. Glownia, T. Katayama, P. Kirchmann, D. Leuenberger, H. Liu, D. Reis, Z. Shen, D. Zhu, Ultrafast formation of domain walls of a charge density wave in $SmTe_3$, Phys. Rev. B 103 (2021) 054109, https://link.aps.org/doi/10.1103/PhysRevB.103.054109.

[18] A. Zong, P. Dolgirev, A. Kogar, Y. Su, X. Shen, J. Straquadine, X. Wang, D. Luo, M. Kozina, A. Reid, R. Li, J. Yang, S. Weathersby, S. Park, E. Sie, P. Jarillo-Herrero, I. Fisher, X. Wang, E. Demler, N. Gedik, Role of equilibrium fluctuations in light-induced order, Phys. Rev. Lett. 127 (2021) 227401, https://link.aps.org/doi/10.1103/PhysRevLett.127.227401.

[19] A. Singh, M. Bachmann, J. Sanchez, A. Pandey, A. Kapitulnik, J. Kim, P. Ryan, S. Kivelson, R. Ian, Fisher emergent tetragonality in a fundamentally orthorhombic material, Sci. Adv. 10 (2024) eadk3321, https://www.science.org/doi/abs/10.1126/sciadv.adk3321.

[20] A. Gallo-Frantz, V. Jacques, A. Sinchenko, D. Ghoneim, L. Ortega, P. Godard, P. Renault, A. Hadj-Azzem, J. Lorenzo, P. Monceau, D. Thiaudière, P. Grigoriev, E. Bellec, D.Le. Bolloc'h, Charge density waves tuned by biaxial tensile stress, Nat. Commun. 15 (2024) 3667, http://dx.doi.org/10.1038/s41467-024-47626-5.

[21] S. Kim, G. Orenstein, A. Singh, I. Fisher, D. Reis, M. Trigo, Emergent symmetry in $TbTe_3$ revealed by ultrafast reflectivity under anisotropic strain, Rep. Progr. Phys. 87 (2024) 100501, http://dx.doi.org/10.1088/1361-6633/ad71ee.

[22] S. Lei, J. Lin, Y. Jia, M. Gray, A. Topp, G. Farahi, S. Klemenz, T. Gao, F. Rodolakis, J. McChesney, C. Ast, A. Yazdani, K. Burch, S. Wu, N. Ong, M. Leslie, Schoop high mobility in a van der Waals layered antiferromagnetic metal, Sci. Adv. 6 (2020) http://dx.doi.org/10.1126/sciadv.aay6407, eaay6407.

[23] I. Gonzalez-Vallejo, V. Jacques, D. Boschetto, G. Rizza, A. Hadj-Azzem, J. Faure, D. Le Bolloc'h, Time-resolved structural dynamics of the out-of-equilibrium charge density wave phase transition in $GdTe_3$, Struct. Dyn. 9 (2022) 1–9, http://dx.doi.org/10.1063/4.0000131.

[24] S. Lee, E. Kim, J. Bang, J. Park, C. Kim, D. Wulferding, D. Cho, Melting of unidirectional charge density waves across twin domain boundaries in GdT_3, Nano Lett. 23 (2023) 11219–11225, https://pubs.acs.org/doi/10.1021/acs.nanolett.3c03721.

[25] R. Costantini, M. Stredansky, D. Cvetko, G. Kladnik, A. Verdini, P. Sigalotti, F. Cilento, F. Salvador, A.De. Luisa, D. Benedetti, L. Floreano, A. Morgante, A. Cossaro, M. Dell'Angela, ANCHOR-SUNDYN: A novel endstation for time resolved spectroscopy at the ALOISA beamline, J. Electron Spectrosc. Relat. Phenom. 229 (2018) 7–12, http://dx.doi.org/10.1016/j.elspec.2018.09.005.

[26] R. Pollak, H. Hughes, Charge density wave phase transitions observed by X-ray photoemission, Le J. de Phys. Colloq. 37 (1976) C4–151–C4–155, http://www.edpsciences.org/10.1051/jphyscol:1976423.

[27] S. Hellmann, M. Beye, C. Sohrt, T. Rohwer, F. Sorgenfrei, H. Redlin, M. Kalläne, M. Marczynski-Bühlow, F. Hennies, M. Bauer, A. Föhlisch, L. Kipp, W. Wurth, K. Rossnagel, Ultrafast melting of a charge-density wave in the Mott insulator 1T TaS2, Phys. Rev. Lett. 105 (2010) 187401, http://dx.doi.org/10.1103/PhysRevLett.105.187401.

[28] S. Hellmann, C. Sohrt, M. Beye, T. Rohwer, F. Sorgenfrei, M. Marczynski-Bühlow, M. Kalläne, H. Redlin, F. Hennies, M. Bauer, A. Föhlisch, L. Kipp, W. Wurth, K. Rossnagel, Time-resolved X-ray photoelectron spectroscopy at FLASH, New J. Phys. 14 (2012) 013062, http://dx.doi.org/10.1088/1367-2630/14/1/013062.

[29] N. Sorgenfrei, E. Giangrisostomi, D. Kühn, R. Ovsyannikov, A. Föhlisch, Time and angle-resolved time-of-flight electron spectroscopy for functional materials science, Molecules 27 (2022) 8833, https://www.mdpi.com/1420-3049/27/24/8833.

[30] S. Sarkar, V. Singh, P. Sadhukhan, A. Pariari, S. Roy, P. Mandal, S. Barman, X-ray photoelectron spectroscopy study of a layered tri-chalcogenide system $LaTe_3$, AIP Conf. Proc. 2220 (2020) 10–14, http://dx.doi.org/10.1063/5.0001764.

[31] S. Seong, H. Kim, K. Kim, B. Min, Y. Kwon, S. Han, B. Park, R. Stania, Y. Seo, J. Kang, Angle-resolved photoemission spectroscopy study of a system with a double charge density wave transition: $ErTe_3$, Phys. Rev. B 104 (2021) 1–9, http://dx.doi.org/10.1103/PhysRevB.104.195153.

[32] S. Seong, E. Lee, Y. Kwon, B. Min, J. Denlinger, B. Park, J. Kang, Angle-resolved photoemission spectroscopy study of rare-earth tritelluride charge density wave compounds: RTe_3 (R=Pr, Er), Electron. Struct. 3 (2021) 024003, https://iopscience.iop.org/article/{10}.1088/{2516}-1075/{{abfeb1}}.

[33] N. Ru, I. Fisher, Thermodynamic and transport properties of YTe_3, $LaTe_3$ and $CeTe_3$, Phys. Rev. B 73 (2006) 033101, https://link.aps.org/doi/10.1103/PhysRevB.73.033101.

[34] E. Ferrari, L. Galli, E. Miniussi, M. Morri, M. Panighel, M. Ricci, P. Lacovig, S. Lizzit, A. Baraldi, Layer-dependent Debye temperature and thermal expansion of Ru(0001) by means of high-energy resolution core-level photoelectron spectroscopy, Phys. Rev. B 82 (2010) 16–21, http://dx.doi.org/10.1103/PhysRevB.82.195420.

[35] S. Hellmann, K. Rossnagel, M. Marczynski-Bühlow, L. Kipp, Vacuum space-charge effects in solid-state photoemission, Phys. Rev. B 79 (2009) 035402, https://link.aps.org/doi/10.1103/PhysRevB.79.035402.

[36] M. Dell'Angela, T. Anniyev, M. Beye, R. Coffee, A. Föhlisch, J. Gladh, S. Kaya, T. Katayama, O. Krupin, A. Nilsson, D. Nordlund, W. Schlotter, J. Sellberg, F. Sorgenfrei, J. Turner, H. Öström, H. Ogasawara, M. Wolf, W. Wurth, Vacuum space charge effects in sub-picosecond soft X-ray photoemission on a molecular adsorbate layer, Struct. Dyn. 2 (2015) 025101, http://dx.doi.org/10.1063/1.4914892.

[37] P. Dutta, S. Chandra, I. Maria, K. Debnath, D. Rawat, A. Soni, U. Waghmare, K. Biswas, Lattice instability induced concerted structural distortion in charged and van der Waals layered $GdTe_3$, Adv. Funct. Mater. 34 (2024) 2312663, https://onlinelibrary.wiley.com/doi/abs/10.1002/adfm.202312663.